

# Ethylene-Mediated Programmed Cell Death during Maize Endosperm Development of Wild-Type and *shrunk2* Genotypes<sup>1</sup>

Todd E. Young, Daniel R. Gallie, and Darleen A. DeMason\*

Departments of Botany and Plant Sciences (T.E.Y., D.A.D.), and Biochemistry (D.R.G.), University of California, Riverside, California 92521-0129

We characterized the progression of programmed cell death during maize (*Zea mays* L.) endosperm development of starchy (*Su*; wild-type) and *shrunk2* (*sh2*) genotypes and tested the involvement of ethylene in mediating this process. Histological and viability staining demonstrated that endosperm cell death was initiated earlier and progressed more rapidly in *sh2* endosperm compared with *Su* endosperm. Internucleosomal DNA fragmentation accompanied endosperm cell death and occurred more extensively in *sh2* endosperm. 1-Aminocyclopropane-1-carboxylic acid levels peaked approximately 16 d after pollination (dap) in *Su* endosperm and gradually decreased during subsequent development, whereas two large 1-aminocyclopropane-1-carboxylic acid peaks were observed in *sh2* endosperm, the first between 16 and 20 dap and the second at 36 dap. Ethylene levels were elevated in *sh2* kernels compared with *Su* kernels, with an initial peak 20 dap approximately 3-fold higher than in *Su* kernels and a second peak 36 dap approximately 5-fold higher than that in *Su* kernels. Ethylene treatment of *Su* kernels resulted in earlier and more extensive endosperm cell death and DNA fragmentation. Aminoethoxyvinylglycine treatment of *sh2* kernels reduced the extent of DNA fragmentation. We conclude that ethylene is involved in triggering programmed cell death in developing maize endosperm and is responsible for the aberrant phenotype of *sh2* kernels.

pcd is an integral part of the development of all multicellular organisms, and the concept of a genetically determined program orchestrating this process has been shown to be functionally conserved among humans, nematodes, and insects (Tomei and Cope, 1991, 1994; Gerschenson and Totello, 1992; Hengartner and Horvitz, 1994). Apoptosis, the most common form of cell death in animals, is characterized by cells actively directing their own death and differs from necrosis, which is not an active, gene-dependent form of death but, rather, results from severe injury to cells (Kerr et al., 1995). Condensation and fragmentation of the nucleus, membrane blebbing, cytoplasmic

condensation, orderly internucleosomal fragmentation of the DNA, and fragmentation of the cell into distinct membrane-bound apoptotic bodies are all characteristics associated with apoptosis (Wyllie, 1980; Earnshaw, 1995; Kerr et al., 1995). Internucleosomal DNA cleavage is catalyzed by endogenous Ca<sup>2+</sup>-dependent endonucleases to generate a ladder of DNA fragments in multiples of approximately 180 to 200 bp (Collins et al., 1992) and is considered to be one hallmark of apoptosis (Wyllie et al., 1984; Wyllie, 1995).

Comparatively little is known about the mechanism(s) underlying pcd in plants or the extent of its functional conservation with animals (Greenberg, 1996; Ryerson and Heath, 1996). Examples of pcd in plants include autolysis of the xylem during differentiation (Chasen, 1994; Wang et al., 1996a), the progression of root cap cells (Wang et al., 1996a; Esau, 1977), the hypersensitive response of resistant plants to pathogen attack (Dietrich et al., 1994; Greenberg et al., 1994; Lamb, 1994; Levine et al., 1996; Wang et al., 1996a), and lysogenic aerenchyma formation in maize (*Zea mays* L.) roots following exposure to hypoxic conditions (Drew et al., 1979; He et al., 1996). Many authors have suggested parallels between pcd in plants and apoptosis in animals (Bachmair et al., 1990; Greenberg and Ausubel, 1993; Dietrich et al., 1994; Greenberg et al., 1994; Lamb, 1994; Greenberg, 1996; Levine et al., 1996; Wang et al., 1996a, 1996b). Genes known to regulate apoptosis have been identified in both nematodes and humans. However, only one animal homolog (*dad1*) has been identified in plants and its function remains to be determined (Apte et al., 1995; Sugimoto et al., 1995).

Cereal endosperm is composed of storage, transfer, and aleurone cells, each of which has a distinctive structural and physiological role in the overall development of this storage tissue (Lopes and Larkins, 1993). The majority of endosperm tissue is composed of storage cells that synthesize starch and storage proteins as a reserve to support growth of the seedling following germination. Aleurone cells play an important role in the mobilization of the stored reserves in the endosperm during germination. During cereal kernel development, starchy endosperm cells die, leaving the cells of the aleurone layer at the endosperm

<sup>1</sup> This study is a portion of a PhD dissertation by T.E.Y. at the University of California, Riverside. This work was partially supported by a Division of Agricultural and Natural Resources grant from the California Agricultural Experiment Station (to D.A.D.) and a U.S. Department of Agriculture National Research Initiative Competitive Grants program grant (no. 95-37100-1618 to D.R.G.).

\* Corresponding author; e-mail demason@ucr1.ucr.edu; fax 1-909-787-4437.

Abbreviations: AVG, aminoethoxyvinylglycine; CEPA, 2-chloroethylphosphonic acid (ethephon); dap, days after pollination; pcd, programmed cell death.

periphery as the only living endosperm cells (Kyle and Styles, 1977; Kowles and Phillips, 1988; Lopes and Larkins, 1993; DeMason, 1994). The causes and progression of endosperm cell death have not been characterized.

A number of maize endosperm mutations have been identified and shown to produce qualitative and/or quantitative differences in carbohydrate metabolism during kernel development, including mutations deficient in starch synthesis, which are currently used for the production of sweet corn (Boyer and Shannon, 1983; Douglass et al., 1993; Azanza et al., 1996). The most commonly used mutation, *sugary1* (*su1*), is characterized by reduced levels of the starch-debranching enzyme, which results in a 2-fold elevation in sugar content (Pan and Nelson, 1984; James et al., 1995). *shrunk2* (*sh2*) encodes one of the subunits for the enzyme ADP-Glc pyrophosphorylase, and mutations in this gene result in kernels with a 2-fold elevation in sugar content over *su1* and a greatly reduced starch content (Creech, 1965; Hannah and Nelson, 1976; Bhave et al., 1990). The *sugary enhancer1* (*se1*) gene is a recessive modifier of the *su1* endosperm mutation and increases total sugar in *su1* kernels to levels comparable to those found in *sh2* kernels (Gonzales et al., 1976; Ferguson et al., 1979).

A number of common pleiotropic effects are manifested during endosperm development in these starch-deficient mutants, including reduced endosperm to embryo ratios, reduced storage protein synthesis, and a characteristic shrunk kernel phenotype at maturity (Tsai et al., 1978; Wann, 1980; Styer and Cantliff, 1983; Harris and DeMason, 1989; Azanza et al., 1996). Additionally, it has been reported that endosperm cells of the starch-deficient maize mutant *shrunk1* (*sh1*) undergo premature cell degeneration during development (Chen and Chourey, 1989; Chourey et al., 1991). Despite the potential significance of these observations, very little progress has been made toward understanding the physiological basis of these pleiotropic effects or their relevance in advancing our understanding of fundamental aspects of cereal endosperm development.

Ethylene is one of the many hormones that have been shown to direct profound effects on growth and development of higher plants, and it has been implicated in a number of diverse processes such as the promotion of seed germination, diageotropism, fruit ripening, pathogenesis, leaf abscission, and flower senescence (Mattoo and Suttle, 1991; Abeles et al., 1992; Fluhr and Mattoo, 1996). More recently, ethylene has also been implicated as part of the signal transduction pathway resulting in *pcd* during the hypersensitive response following pathogen attack (Ward et al., 1991; Greenberg et al., 1994) and the formation of lysogenic aerenchyma in maize roots in response to exposure to hypoxic conditions (Drew et al., 1979; Campbell and Drew, 1983; He et al., 1996). Furthermore, Beltrano et al. (1994) showed that ethylene is synthesized during wheat ear development and that ethylene application hastens the process of grain maturation, whereas treatment with ethylene biosynthesis inhibitors had the opposite effect.

In light of these observations we hypothesized that ethylene may be responsible for the premature death and collapse of the central endosperm of the various starch-

deficient mutants as a consequence of the stress resulting from the elevated sugar levels. The objectives of this study were (a) to compare the progression of cell death in the developing endosperm of *Su* and *sh2* genotypes of maize by characterizing histological and viability changes, (b) to correlate these changes with the progression of DNA fragmentation and induction of nuclease activity, (c) to determine whether ethylene levels are higher in starch-deficient endosperm mutants, and (d) to establish a causal relationship between ethylene exposure and *pcd* in mutant and wild-type endosperm.

## MATERIALS AND METHODS

The maize (*Zea mays* L.) inbred lines I451b and Oh43, isogenic for the starchy wild-type (*Su* = *Su1Se1*; *Sh2*) and the recessive endosperm mutations *su1*, *su1se1*, and *sh2* were used for this study. Because of poor germination, embryos from I451b *sh2* kernels were first cultured on medium containing 1% (w/v) agar, 3% (w/v) Suc, and Murashige and Skoog salts for 2 to 3 weeks, and the young seedlings were transplanted to the field along with seeds of the remaining genotypes. Plants were hand-pollinated and developing kernels were collected at 4-d intervals from 8 to 48 dap. Three samples collected from three separate ears for each developmental stage were frozen in liquid N<sub>2</sub> and stored at -80°C until analysis.

### Viability Staining

Twenty fresh kernels were collected for *Su* and *sh2* genotypes of I451b at developmental stages ranging from 12 to 44 dap at 4-d intervals. Near-median longitudinal hand sections (approximately 3 mm thick) were stained in 0.1% (w/v) Evans blue (C.I. 23860) for 2 min (Gaff and Okong 'O-Ogola, 1971). Stained sections were washed with water for 30 min and photographed with Kodak T-Max 100 film on a Nikon Multiphot photomacrography system with reflected lighting.

### Histology

Developing kernels of I451b (*Su* and *sh2*) were collected 16, 20, 24, 28, 32, and 40 dap. A 3-mm-thick median longitudinal section was removed from each and fixed in 2% (v/v) glutaraldehyde and 2% (v/v) paraformaldehyde in 50 mM phosphate buffer, pH 7.2, for 7 to 10 d. Samples were then dehydrated through a graded ethanol series, infiltrated with a graded methacrylate (JB-4 plastic, Polysciences, Warrington, PA) series, and finally infiltrated in 100% (v/v) methacrylate at 4°C for approximately 1 year before polymerization. Whole median longitudinal sections, 4 μm in thickness, were made on a retracting rotary microtome (JB-4, Sorvall). Sections were affixed to slides and stained with the periodic acid-Schiff reaction (O'Brien and McCully, 1981) and with aniline blue-black (Fisher, 1968) to detect insoluble carbohydrates and proteins, respectively. Sections were photographed with Kodak Technical Pan 2415 film on a Nikon Multiphot photomacrography system with transmitted lighting.

### DNA Extraction and Fragmentation Analysis

Twenty frozen kernels were ground in liquid N<sub>2</sub> with a mortar and pestle to a fine powder. Eight milliliters of extraction buffer (100 mM Tris-HCl, pH 9.0, 20 mM EDTA, 200 mM NaCl, 1% [w/v] sarcosyl, and 10  $\mu\text{L mL}^{-1}$   $\beta$ -mercaptoethanol) was then added, followed by 8 mL of phenol:chloroform (1:1, v/v), and the samples were ground further. Samples were centrifuged at 8,000g for 15 min and transferred to a new tube, and the total nucleic acid was precipitated from the supernatant by the addition of a 1/10th volume of 3 M sodium acetate, pH 6.0, and an equal volume of isopropanol at  $-20^{\circ}\text{C}$ . The precipitated nucleic acid was dissolved in 1 mL of extraction buffer without vortexing, reprecipitated in sterile 2-mL centrifuge tubes, washed three times with 1 mL of 70% (v/v) ethanol, and dissolved in T<sub>10</sub>E<sub>5</sub> (10 mM Tris-HCl, pH 8.0, and 5 mM EDTA). RNase (DNase-free) was added to a final concentration of 100  $\mu\text{g mL}^{-1}$  and incubated for 1 h at  $37^{\circ}\text{C}$ . Samples were then extracted with an equal volume of phenol:chloroform (1:1, v/v) and centrifuged at 12,000g, and DNA was reprecipitated from the supernatant and dissolved in T<sub>10</sub>E<sub>5</sub>. DNA concentrations were determined spectrophotometrically.

For DNA-fragmentation analysis, 20  $\mu\text{g}$  of each sample was resolved on a 1.8% agarose gel containing 1 $\times$  TBE (90 mM Tris-borate and 0.1 mM EDTA), stained with ethidium bromide, and photographed on a UV light box.

### DNase Activity Assays and Gels

Ten kernels per sample were ground in liquid N<sub>2</sub>. Following the addition of 2 mL of extraction buffer (50 mM Hepes, pH 7.5, 50 mM magnesium acetate, and 1.2 mM potassium acetate) and subsequent grinding, the samples were centrifuged at 12,000g for 10 min. Protein concentration of the supernatant was determined according to the method of Bradford (1976). Three separate extractions were performed for each developmental stage and used for both nuclease activity gels and ACC determination.

To determine total DNase activity present within samples, 10  $\mu\text{g}$  of total endosperm protein or 100  $\mu\text{g}$  of total embryo protein was suspended in assay buffer (100 mM Mops, pH 6.8, 10 mM CaCl<sub>2</sub>, and 10 mM MgCl<sub>2</sub>) to a final volume of 100  $\mu\text{L}$  and placed on ice. Four-hundred microliters of ice-cold DNA solution (500  $\mu\text{g}$  of sheared, denatured herring-sperm DNA suspended in 1 mL of assay buffer) was added to each of the protein samples and mixed. One-hundred microliters of the reaction mixture was removed and placed into a tube containing 400  $\mu\text{L}$  of ice-cold 5% (v/v) perchloric acid and 0.2% (w/v) uranyl acetate and vortexed, and the undigested DNA was precipitated on ice for 15 min. Samples were then centrifuged at 12,000g for 10 min and the supernatant was transferred to a new tube, which served as the 0 time point. The assay tubes were then placed in a  $37^{\circ}\text{C}$  water bath and additional samples (100  $\mu\text{L}$  each) were collected at 1, 2, and 4 h. Undigested DNA was precipitated as described for the 0 time point. The  $A_{260}$  of the supernatant was determined with a UV spectrophotometer and the value of the 0 time

point was subtracted from each of the time points. Activity was expressed as the change in  $A_{260} \text{ mg}^{-1} \text{ protein h}^{-1}$  and represents a mean of three separate assays.

DNase activities were characterized using the substrate-based SDS-PAGE activity according to methods described by Thelen and Northcote (1989) with modifications. For DNase activity gel analysis, protein extracts were diluted to a final concentration of 1  $\text{mg mL}^{-1}$  in 1 $\times$  SDS sample buffer (50 mM Tris, pH 6.8, 2% [w/v] SDS, 0.1% [w/v] bromophenol blue, and 10% [v/v] glycerol). Twenty micrograms of each protein sample were loaded onto a 10% SDS-PAGE gel containing 20  $\mu\text{g mL}^{-1}$  sheared, denatured herring-sperm DNA. Following electrophoresis, the gels were washed three times (10 min/wash) with a solution containing 25% (v/v) isopropanol and 10 mM Tris buffer, pH 7.5, to remove the SDS. The gels were then washed three times (10 min/wash) with 10 mM Tris buffer, pH 7.5, to remove the isopropanol and incubated at  $50^{\circ}\text{C}$  in 100 mM Mops buffer containing 10 mM CaCl<sub>2</sub> and MgCl<sub>2</sub> for 30 min for endosperm nucleases or 1 h for embryo nucleases. The gels were then stained in aqueous ethidium bromide (1  $\mu\text{g mL}^{-1}$ ) for 10 min and destained for 1 h with several changes of water. Gels were photographed on a UV light box. To determine whether these activities were DNases or nucleases, similar activity gel analysis was conducted using RNA as the substrate except that gels were stained in 2% (w/v) aqueous Toluidine blue O for 3 min, destained with several changes of water, and photographed on a light box.

### ACC and Ethylene Determinations

ACC content was determined as described by Concepcion et al. (1979) with modifications. A 200- $\mu\text{L}$  aliquot of protein extract (one kernel equivalent) was diluted with 600  $\mu\text{L}$  of water and 100  $\mu\text{L}$  of 10 mM HgCl<sub>2</sub> in a test tube. The tubes were sealed with a rubber serum stopper and placed on ice, and 100  $\mu\text{L}$  of 5% sodium hypochlorite: saturated NaOH solution (2:1, v/v) was added with a syringe to each before vortexing for 5 s. After the sample was incubated on ice for 1 h, 1 mL of gas was removed with a gas-tight syringe and injected into a gas chromatograph (Autosystem, Perkin-Elmer) equipped with a 45/60 column (Carboxen 1000, Supelco, Bellefonte, PA) and a flame-ionization detector. A set of ACC (Sigma) standards of known concentration was used to calculate a regression equation to determine the ACC content within the samples.

For ethylene determinations fresh kernels were collected at 4-d intervals from 8 to 48 dap. Three samples (10 kernels each) were collected at each stage and placed between moist paper towels for 1 h to reduce potential wounding effects. The kernels were then transferred to tubes and fitted with a rubber serum stopper. Following a 3-h incubation, 1 mL of gas was removed from the tube with a gas-tight syringe and injected into the chromatograph. A set of ethylene standards was used to calculate a regression equation to determine the amount of ethylene generated per kernel per hour.

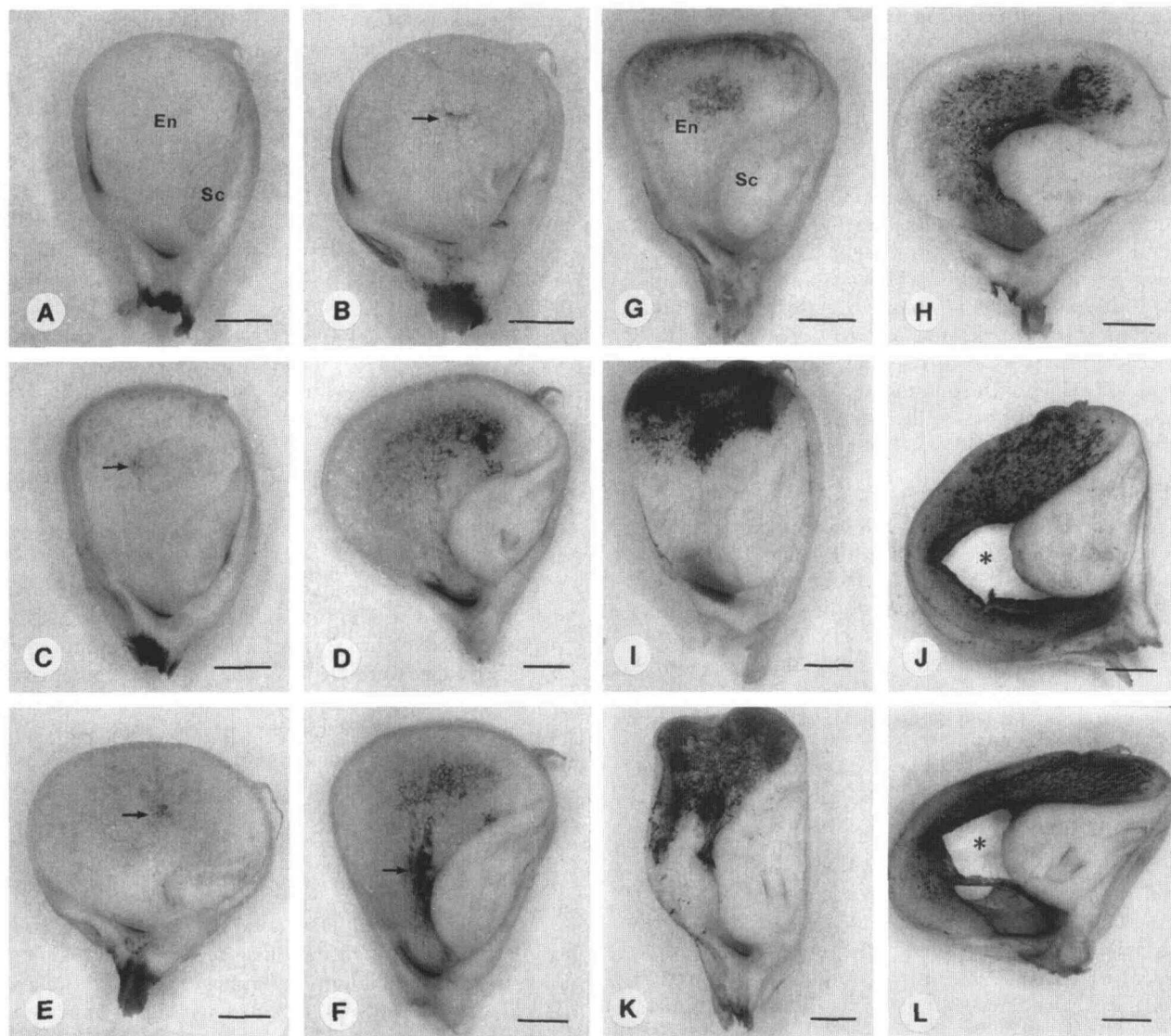


Figure 1. (Figure continues on facing page.)

### Application of Growth Regulators

For ethylene treatments control and test ears of Il451b (*Su*) and Oh43 (*Su* and *sh2*) were covered 20 and 16 dap, respectively, with a 1-L plastic bag and tightly sealed with petroleum jelly and a rubber band to prevent gas escape. One milliliter of ethylene (1% in  $N_2$ ; Scott Specialty Gasses, Plumsteadville, PA) was then added to the bag containing the test ear with a gas-tight syringe to a final concentration of  $10 \mu L L^{-1}$ , and the puncture was sealed with tape. Bags were left on the ear for 24 h. Treatments were reapplied every 2 d, and triplicate samples were collected every 4 d. Samples were used fresh, stained for viability, to determine ethylene evolution, or frozen in liquid  $N_2$  for DNA and protein extractions. Residual kernels of Il451b (*Su*) were allowed to mature fully and were collected 50 dap. Three replicates of 50 mature kernels from both control and ethylene-treated ears were surface-sterilized with a 5%

(v/v) bleach solution, rinsed several times, and soaked for 12 h in sterile water. Kernels were planted in sterile vermiculite and allowed to germinate under greenhouse conditions for 4 weeks, after which the percentage of germination was calculated.

For treatment of control and test ears with either CEPA as an exogenous ethylene source or AVG as an inhibitor of ethylene biosynthesis (Sigma), husks of Oh43 (*sh2*) ears were pulled back and the exposed kernels were treated with 2 mL of solution containing water (as a control), 100 mM CEPA, or 10  $\mu M$  AVG. Husks were then replaced and attached with a rubber band at the tip to prevent premature drying of the developing kernels. Triplicate samples were collected every 4 d, at which times the treatments were repeated. Samples were used fresh to determine ethylene evolution, stained for viability as described above, or frozen in liquid  $N_2$  for DNA and protein extraction.

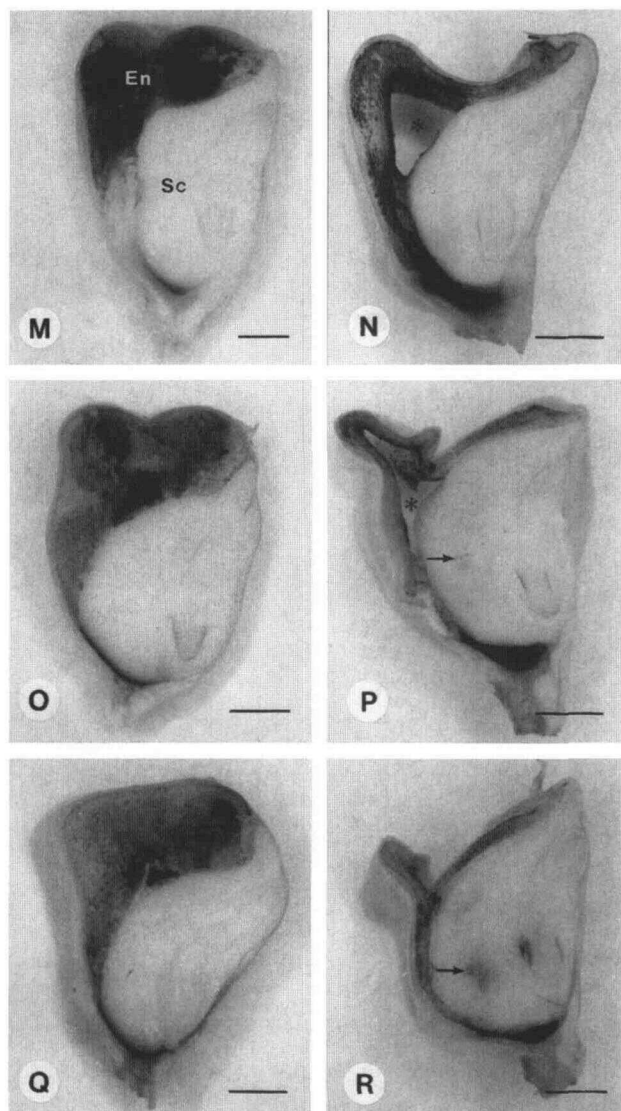


**Figure 1.** (Figure continued from facing page.) Progression of endosperm cell death in *Su* (left) and *sh2* (right) genotypes of Il451b, as indicated by Evans blue staining. Developmental stages shown are: A and B, 12 dap; C and D, 16 dap; E and F, 20 dap; G and H, 24 dap; I and J, 28 dap; K and L, 32 dap; M and N, 36 dap; O and P, 40 dap; and Q and R, 44 dap. In B, C, E, and F, the arrow indicates the initiation of cell death at the central endosperm; in P and R, the arrow indicates scutellum cell death. Asterisks (\*) indicate cavity formation within the central endosperm. En, Endosperm; Sc, scutellum/embryo. Scale bars = 3 mm.

## RESULTS

### Progression of Cell Death during Endosperm Development

The viability of endosperm cells during *Su* and *sh2* kernel development was examined by staining fresh hand sections with Evans blue, a dye that is excluded from living cells with intact plasma membranes, thereby staining only the cytoplasm of nonviable cells. No Evans blue staining of cells within the *Su* endosperm was detected 12 dap (Fig. 1A). Between 16 and 20 dap, a few cells within the central endosperm were stained, indicating loss of viability (Fig. 1,

C and E). By 24 dap, staining within the central endosperm was more prominent and additional staining near the top of the kernel was evident (Fig. 1G). By 28 dap the entire top half of the endosperm, except for the aleurone layer, was stained (Fig. 1I). Further staining proceeded basipetally between 32 and 40 dap (Fig. 1, K, M, and O) until 44 dap (Fig. 1Q), when all starchy endosperm cells were stained.

In contrast to the Evans blue-staining pattern of *Su* kernels, nonviable cells were present within the central endosperm in *sh2* kernels by 12 dap (Fig. 1B) and the extent of staining proceeded more rapidly between 16 and 20 dap (Fig. 1, D and F) than was observed in *Su* endosperm. Additionally, stained, collapsed, and stretched cells adjacent to the basal portion of the scutellum were present (Fig. 1F), which was not observed in the *Su* genotype. By 24 dap the majority of central endosperm cells were stained (approximately 8 d earlier than in the *Su* genotype) and stained cells occurred along the entire length of the scutellum (Fig. 1H). A small cavity resulting from cellular degeneration formed directly adjacent to the scutellum (Fig. 1H). Between 28 and 32 dap the remainder of endosperm cells died, while the cavity within the central endosperm continued to increase in size (Fig. 1, J and L). Between 36 and 44 dap the endosperm collapsed down upon the embryo, resulting in the shrunken kernel phenotype typical of this genotype (Fig. 1, N, P, and R). Patches of nonviable cells were also detected within the scutella of *sh2* kernels starting 40 dap (Fig. 1P) and occurring more extensively by 44 dap (Fig. 1R); this was not observed in the *Su* genotype.

### Histological Characterization of Endosperm Development

In the *Su* genotype starch deposition had started in the upper half of the kernel by 16 dap (Fig. 2A), progressed basipetally through 24 dap (Fig. 2, C and E), and increased through 40 dap (Fig. 2, G, I, and K) until the entire endosperm had filled with starch, with the exception of a few central endosperm cells that degenerated, leaving a small cavity within the center of the kernel (Fig. 2K). Storage protein deposition occurred mainly at the periphery of the kernel starting 16 dap and progressing centrifugally through 40 dap.

The *sh2* kernels 16 to 20 dap were morphologically similar to the *Su* kernels, with the exception of greatly reduced starch deposition (Fig. 2, B and D). Limited starch and storage protein deposition in the *sh2* genotype occurred by 24 dap (Fig. 2F) and increased through 40 dap (Fig. 2, H, J, and L). Additionally, by 24 dap some *sh2* endosperm cells were collapsed and stretched, particularly near the basal portion of the kernel adjacent to the scutellum (Fig. 2F). By 28 dap a cavity had formed within the central endosperm of the *sh2* kernels (Fig. 2H), which increased in size throughout development as the endosperm cells continued to degenerate (Fig. 2, J and L), resulting in a hollow kernel. During desiccation (between 28 and 40 dap) the remaining peripheral endosperm collapsed down upon the embryo, resulting in the typical shrunken phenotype (Fig. 2, H, J, and L).



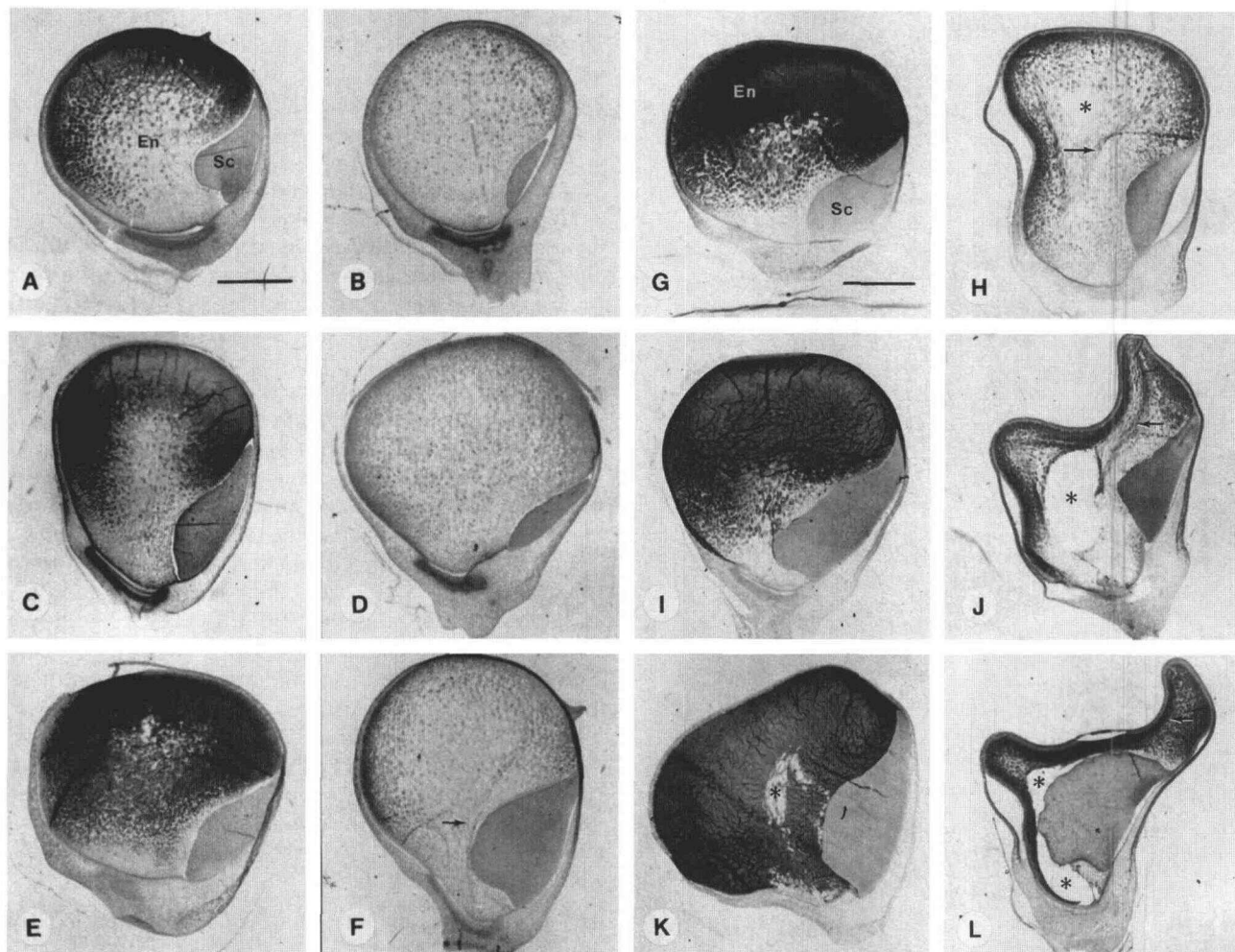


**Figure 2.** Kernel development of *Su* (left) and *sh2* (right) genotypes of Il451b. Developmental stages shown are: A and B, 16 dap; C and D, 20 dap; E and F, 24 dap; G and H, 28 dap; I and J, 32 dap; and K and L, 40 dap. Arrows indicate endosperm cell degeneration and collapse. Asterisks (\*) indicate cavity formation within the central endosperm. En, Endosperm; Sc, scutellum/embryo. Scale bars = 2 mm.

### Internucleosomal DNA Degradation during Endosperm Development

DNA quality was examined during the development of *Su* and *sh2* kernels to determine whether internucleosomal fragmentation accompanied endosperm cell death. The appearance of a ladder of DNA cleavage products was evident in both the *Su* and *sh2* genotypes of Il451b by 28 dap (Fig. 3). The patterns of DNA fragmentation were similar for both the whole-kernel and endosperm samples, except that the extent of cleavage was more pronounced in the latter. The progression of endosperm DNA fragmentation was gradual in *Su* relative to that in *sh2* endosperm, where it occurred more rapidly over a shorter period of development. By 32 dap most of the DNA in *sh2* endosperm had been digested into 180- to 200-bp fragments, whereas internucleosomal cleavage was much less extensive in *Su* endosperm at this same developmental stage. A slight amount of DNA fragmentation was observed at 8 dap for both the *Su* and *sh2* genotypes. Additionally, DNA fragmentation was present in *sh2* embryos at low levels

throughout development but more extensively between 40 and 44 dap; no detectable fragmentation was observed in *Su* embryos. Similar results were observed for the *Su* and *sh2* genotypes of Oh43 except that no fragmentation was seen in the *sh2* embryos of this background (data not shown).

### Nuclease Activity and Activity Gel Analysis

Nuclease activity in the endosperm and scutellum of developing kernels was determined to establish whether the internucleosomal degradation of the DNA during endosperm development is accompanied by changes in nuclease expression. High levels of total nuclease activity were present in the endosperm of both *Su* and *sh2* genotypes of Il451b between 8 and 12 dap, which sharply declined to low levels by 24 dap (Fig. 4A). Nuclease activity then increased from 24 to 36 dap and the levels were approximately 50 to 75% greater in the *sh2* endosperm. Nuclease activity gel analysis revealed three active nucle-

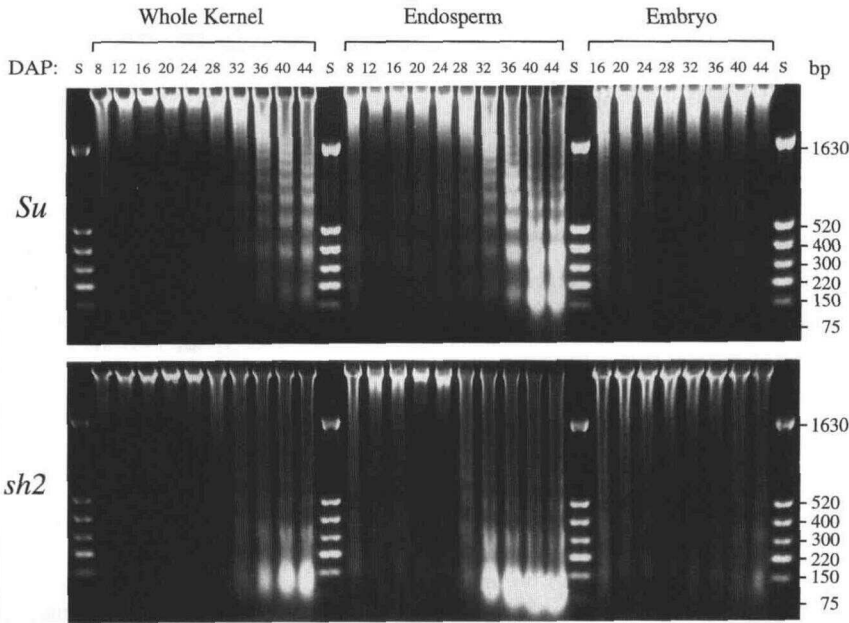


**Figure 3.** DNA-fragmentation analysis of whole kernel, endosperm, and embryo during development of *Su* and *sh2* kernels of I451b. Sizes (bp) of markers (lanes S) are indicated.

ases with masses of 33.5, 36.0, and 38.5 kD in both genotypes (Fig. 4B). Activities of the same size were also present in activity gels when RNA was used as the substrate and were significantly reduced when EDTA was included in the incubation buffer (data not shown). During early endosperm development similar nucleases were present in both genotypes, with the 33.5-kD nuclease being the most active between 8 and 12 dap and then gradually decreasing through 24 dap. Between 24 and 44 dap the 33.5-kD nucle-

ase and, to a lesser extent, the 36.0-kD nuclease increased in activity more rapidly in the endosperm of the *sh2* genotype. The 38.5-kD nuclease was less active at all stages of development in both genotypes.

Total nuclease activity was approximately 10-fold lower in the embryo compared with the endosperm (Fig. 4C). In the *Su* genotype activity was low 16 to 20 dap, gradually increased through 36 dap, and then decreased to low levels between 36 and 44 dap. Similar results were observed in

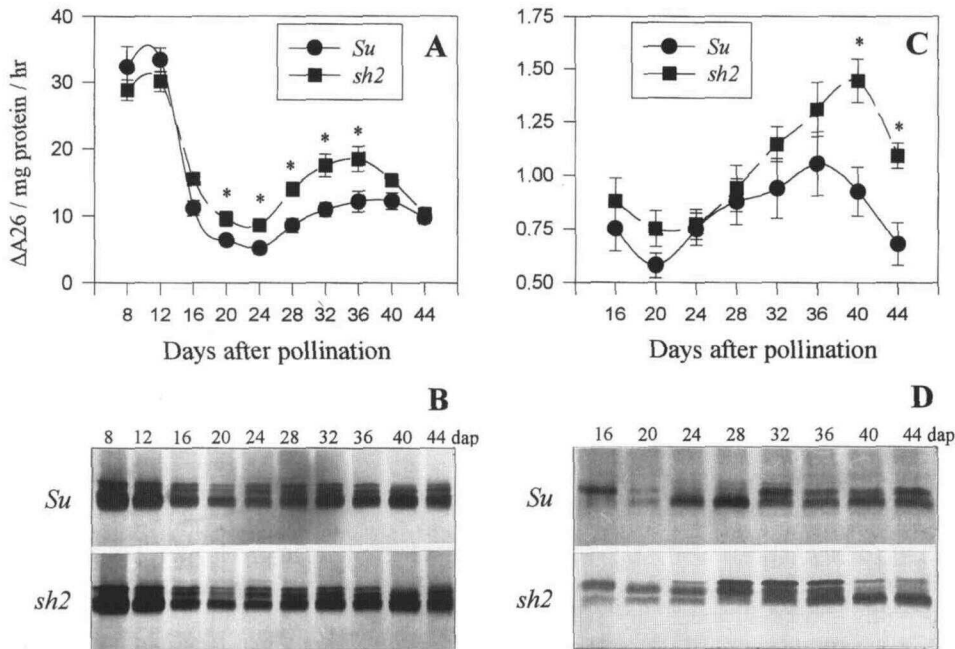


**Figure 4.** Nuclease activity in endosperm and embryo during development of *Su* and *sh2* kernels of I451b isogenic lines. Total endosperm (A) and embryo (C) nuclease activities were determined using in vitro assays; each data point is the average  $\pm$  SD of three replicates. Nuclease activity profiles of endosperm (B) and embryo (D) were determined using activity gels. Asterisks (\*) indicate significant differences between the *Su* and *sh2* genotypes ( $P < 0.05$ ).

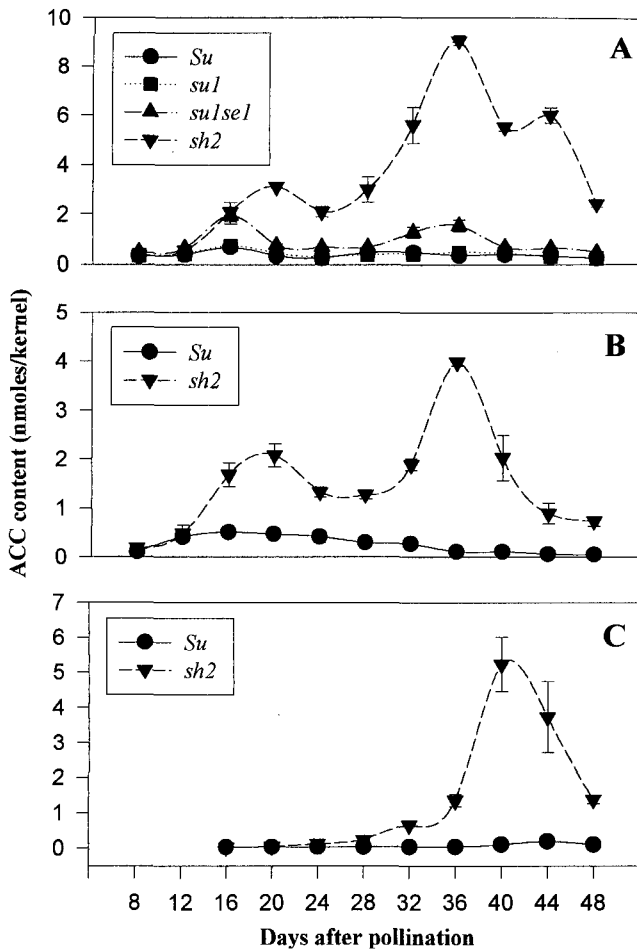


**Figure 5.** ACC content in Il451b isogenic lines during development. A, Whole kernels; B, endosperm; and C, embryo. Each data point is the average  $\pm$  SD of three replicates.

the *sh2* embryo, except that between 40 and 44 dap the activity was approximately 50% greater than in the *Su* genotype. The nuclease activity profiles in *Su* and *sh2* embryos were comparable throughout development, with a gradual switch from higher-molecular-mass forms during early development to lower-molecular-mass forms during later development (Fig. 4D). Between 28 and 36 dap the 38.5-kD nuclease was more prominent in the *sh2* embryo, whereas between 40 and 44 dap the 33.5-kD nuclease was primarily responsible for the differences in total activity between the *Su* and *sh2* embryos.

#### ACC Content and Ethylene Production

As a first step toward establishing a link between ethylene and premature endosperm cell death in the *sh2* mutant, we determined the levels of ACC, an intermediate in the ethylene biosynthesis pathway. Significantly higher levels of ACC were present in *sh2* kernels and, to a lesser extent, in *su1se1* kernels compared with *Su* and *su1* kernels (Fig. 5A). Two peaks of ACC were detected in the high-sugar mutants; the first occurred at approximately 16 to 20 dap and the second occurred at approximately 32 to 36 dap. The

two peaks were approximately the same in the *su1se1* kernels; however, the second peak in the *sh2* genotype was approximately 3-fold higher than the first. A single small peak of ACC was also present in the *Su* and *su1* kernels at 16 dap.

ACC levels within the endosperm and embryo were measured separately for the *Su* and *sh2* genotypes to determine the location of ACC within the kernel. In *Su* endosperm the ACC levels peaked at approximately 16 dap and gradually decreased during subsequent development (Fig. 5B). In contrast, two ACC peaks occurred in the *sh2* endosperm, the first between 16 and 20 dap and the second at 36 dap, with the second peak approximately 2-fold higher than the first. This is similar to what was observed for whole *sh2* kernels, except that the second peak was approximately 3-fold higher than the first. In *Su* embryos ACC levels remained low throughout development. In *sh2* embryos ACC content peaked 40 dap and then decreased to a low level by 48 dap (Fig. 5C). The majority of ACC was found in the endosperm of both genotypes at early stages of development, whereas at later stages of development, there were approximately equal amounts present in both the endosperm and embryo of the *sh2* genotype.

To determine whether the observed differences in ACC synthesis resulted in differences in ethylene production, the rate of ethylene production was determined for developing kernels of the same isogenic lines of Il451b. Initial rates on a per kernel basis were similar for all of the genotypes and decreased to low levels by 24 dap (Fig. 6A). However, by 16 dap ethylene production rates for the *sh2* and *su1se1* genotypes were approximately 2- to 3-fold higher than those of the *Su* and *su1* genotypes. There was also a second ethylene peak in all genotypes, but the timing and extent in each differed significantly. In *Su* kernels there was a gradual increase in ethylene production, which peaked approximately 36 dap and then declined gradually through 48 dap. In *sh2* kernels the rate increased very rapidly after 24 dap, peaked approximately 36 dap to a level about 5-fold higher than that in *Su* kernels, and then rapidly declined to a low level by 44 dap. Ethylene production rates in *su1* and *su1se1* kernels were intermediate between those measured in *Su* and *sh2* kernels. Ethylene levels in *su1se1* kernels increased more quickly during development than those in *su1* kernels. Ethylene production in both *su1* and *su1se1* kernels peaked a second time by 40 dap and then gradually decreased by 44 dap.

Ethylene production was also determined for the *Su* and *sh2* genotypes in the Oh43 inbred background for comparison. We observed a number of similarities between these two inbred backgrounds, including the occurrence of two peaks in ethylene production during development and higher ethylene production rates in the *sh2* genotype (Fig. 6B). However, in the Oh43 background the absolute rates of ethylene production were higher than those observed in Il451b, which can in part be accounted for by its larger kernel size (approximately 33% larger, data not shown). Furthermore, the difference in ethylene production between the *Su* and *sh2* genotypes of Oh43 was considerably less (approximately 2-fold) than that between *Su* and *sh2*



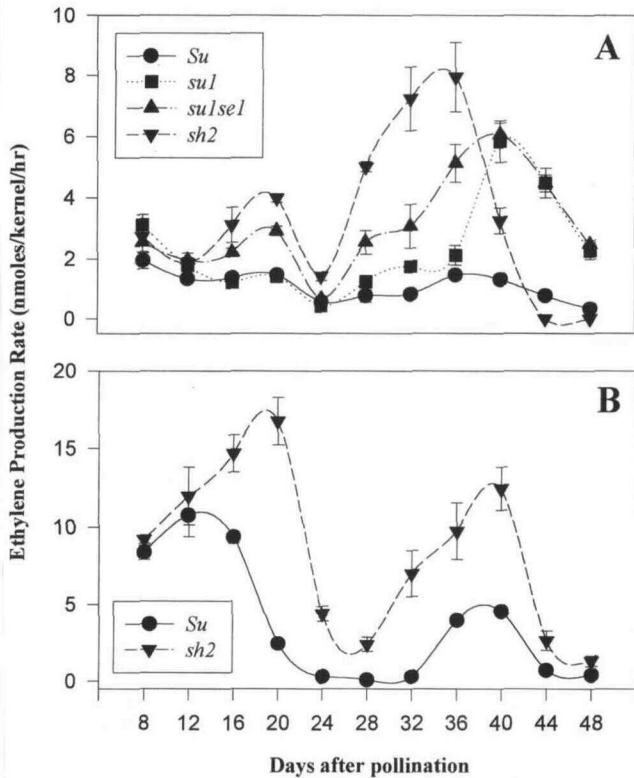


**Figure 6.** Ethylene production during development. A, Il451b isogenic line; B, Oh43 isogenic line. Each data point is the average  $\pm$  SD of three replicates.

(approximately 5-fold) in Il451b, and the first peak of ethylene in Oh43 was higher than the second.

**Ethylene Treatment of Developing Kernels**

To establish a causal relationship between elevated ethylene production and premature endosperm cell death during *sh2* kernel development, developing *Su* and *sh2* kernels were exposed to exogenous ethylene and examined for effects on initiation of endosperm cell death and internucleosomal DNA cleavage. Kernels of Oh43 (*Su*) that were exposed to  $10 \mu\text{L L}^{-1}$  ethylene 16 dap showed more extensive endosperm cell death by 20 dap relative to the control (Fig. 7, A and B). At 24 and 28 dap the progression of cell death continued more rapidly in the ethylene-treated endosperm (data not shown). Ethylene treatment also caused endosperm collapse, but in contrast to normal *sh2* endosperm development, the endosperm collapsed from the periphery toward the center. Coincident with the premature onset of cell death of ethylene-treated endosperm was an accelerated induction of DNA fragmentation (Fig. 7C). DNA fragmentation was observed by 20 dap and had progressed to a greater extent by 24 to 28 dap than in control kernels. Similar effects were observed for the *sh2* genotype.

Kernels of Il451b (*Su*) that were exposed to  $10 \mu\text{L L}^{-1}$  ethylene treatments 20 dap showed more extensive endosperm cell death, similar to what was observed for Oh43 *Su* kernels (data not shown), as well as extensive cell death

in the scutellum by 32 dap relative to the control (Fig. 8, A and B). Furthermore, endosperm and scutellum sizes were significantly reduced for the ethylene-treated kernels (Fig. 8, A and B). Premature induction of DNA fragmentation occurred more rapidly in the ethylene-treated kernels compared with the control (Fig. 8C), similar to results observed in the Oh43 inbred (Fig. 7C). Furthermore, ectopic induction of DNA fragmentation was observed in embryos of the ethylene-treated kernels by 36 dap (Fig. 8C), which was not observed in control kernels. The mature dry weight of control kernels ( $121.6 \pm 3.02 \text{ mg}^{-1}$  kernel) was significantly higher than that of ethylene-treated kernels ( $91.53 \pm 1.03$

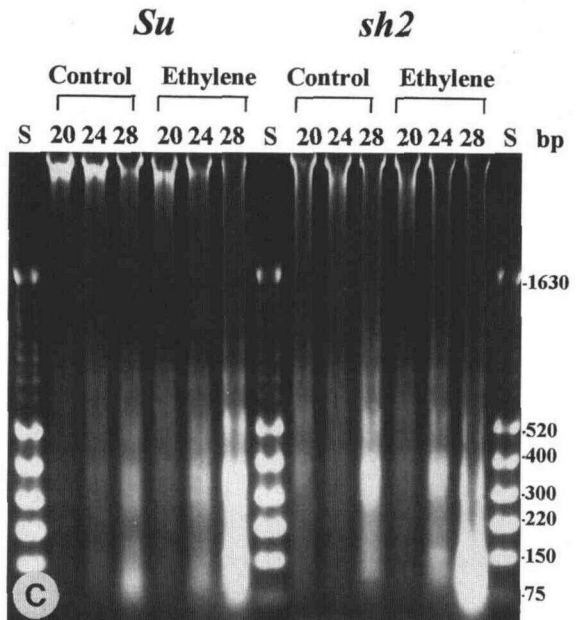
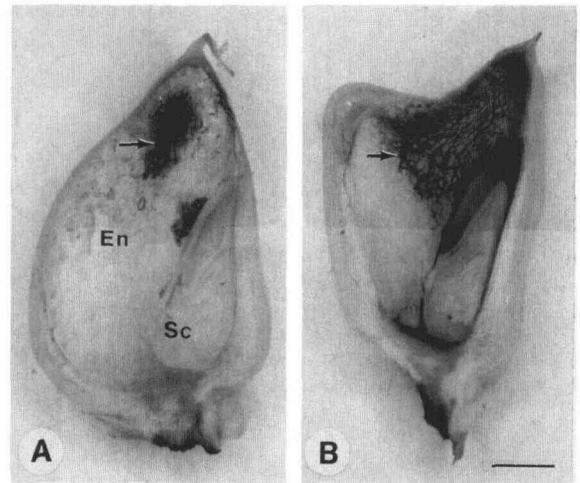


**Figure 7.** Effects of ethylene on kernel development of Oh43 isogenic lines. Viability in control (A) and ethylene-treated (B) kernels of Oh43 (*Su*) at 20 dap (4 d after treatment). Arrows indicate dead cells in the endosperm. En, Endosperm; Sc, scutellum/embryo. Scale bar = 3 mm. C, DNA-fragmentation analysis (whole kernels) of *Su* and *sh2* kernels following control and ethylene treatment initiating 16 dap. Sample times are in dap. Sizes (bp) of markers (lanes S) are indicated.

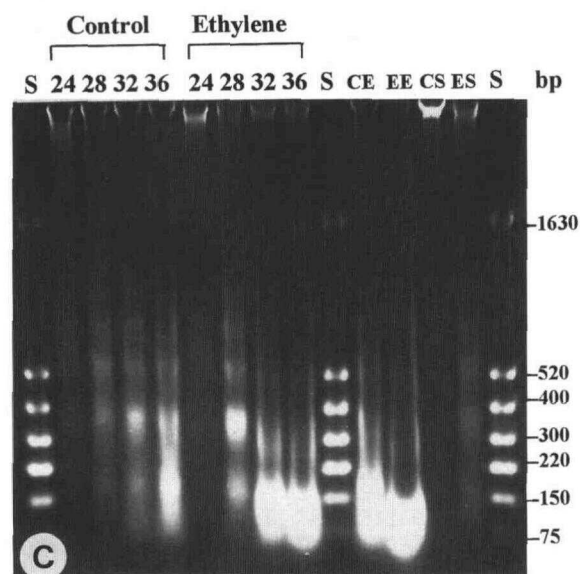
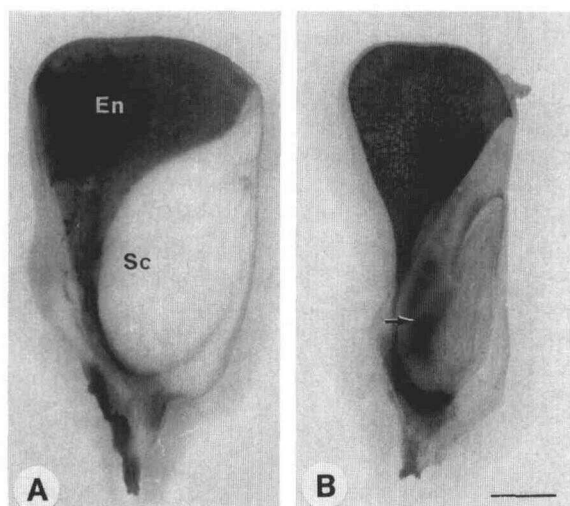


**Figure 8.** Effects of ethylene on Il451b (*Su*) kernel development. Kernel viability in control (A) versus ethylene-treated (B) kernels at 32 dap (12 d after treatment). The arrow indicates dead cells in the scutellum. En, Endosperm; Sc, scutellum/embryo. Scale bar = 3 mm. C, DNA-fragmentation analysis during development of whole kernels following control and ethylene treatment. CE, Endosperm of control kernels; EE, endosperm of ethylene-treated kernels; CS, scutellum of control kernels; and ES, scutellum of ethylene-treated kernels 36 dap. Treatments were initiated 20 dap and sample times are in dap. Sizes (bp) of markers (lanes S) are indicated.

mg<sup>-1</sup> kernel;  $P \leq 0.002$ ). Moreover, these ethylene-treated kernels exhibited significantly reduced germination ( $5.33 \pm 3.06\%$ ) compared with control kernels ( $94.67 \pm 1.15\%$ ;  $P < 0.00001$ ).

To obtain further evidence for a role of ethylene in mediating pleiotropic effects during *sh2* kernel development, kernels of the Oh43 *sh2* (16 dap) were exposed to either 10  $\mu$ M AVG to inhibit endogenous ethylene biosynthesis or 100 mM CEPA to serve as additional verification of the ethylene-induced effects. By 28 dap control kernels

showed extensive endosperm cell death and the formation of a central cavity (Fig. 9A), similar to what was observed for Il451b *sh2* kernels (Fig. 2J) at the same stage. CEPA treatment also resulted in more extensive endosperm cell death and collapse of the endosperm away from the pericarp (Fig. 9B).

The application of AVG did not appear to reduce the extent of cell death significantly; however, it did inhibit the formation of a central cavity (Fig. 9C). In control kernels extensive DNA fragmentation was observed by 28 dap (Fig. 9D). Treatment with CEPA resulted in premature induction of DNA fragmentation by 24 dap, whereas AVG-treated kernels exhibited less extensive DNA fragmentation than did control kernels (Fig. 9D). Ethylene production rates following exogenous application of AVG were approximately 20% of control kernels, indicating that these applications were effective in reducing ethylene biosynthesis but were not sufficient to completely inhibit production.

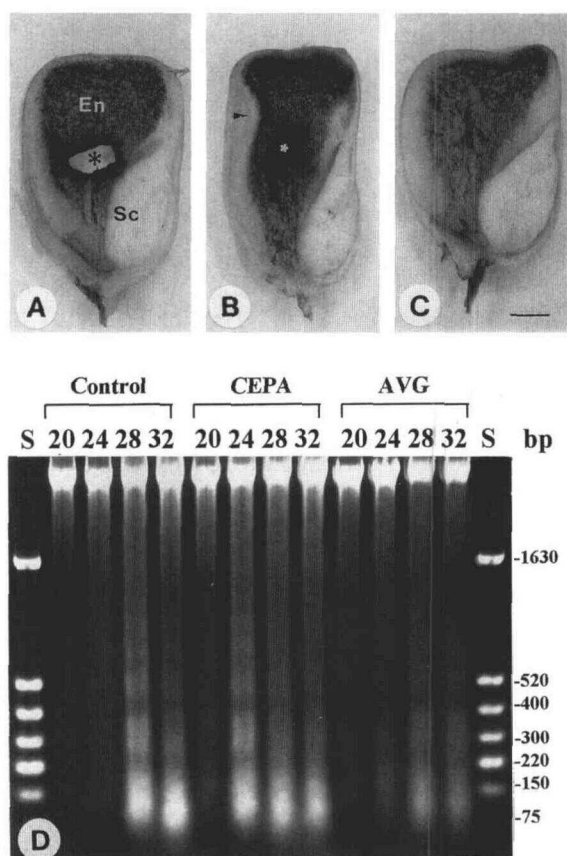


**Figure 9.** Ethylene effects on Oh43 (*sh2*) kernel development. Kernel viability in control (A), CEPA-treated (B), and AVG-treated (C) kernels at 28 dap (12 d after treatment). The arrowhead indicates collapse of the endosperm away from the seed coat. Asterisks (\*) indicate cavity position within the central endosperm, which is obscured by section thickness in B. En, Endosperm; Sc, scutellum/embryo. Scale bar = 3 mm. D, DNA-fragmentation analysis of whole kernels following control, CEPA, and AVG treatments at 16 dap. Sample times are in dap. Sizes (bp) of markers (lane S) are indicated.

## DISCUSSION

Late in cereal endosperm development a cell death program is initiated, but the progression or causes of this process have not been studied. The focus of this study was to characterize maize endosperm cell death and identify key differences related to premature endosperm degeneration of the starch-deficient *sh2* mutant. As a result of our findings we conclude that (a) maize endosperm cell death is a developmentally controlled process that involves internucleosomal DNA cleavage, and (b) ethylene is the signal responsible for mediating pleiotropic effects associated with *sh2* kernel development and is involved in the signal transduction pathway leading to endosperm *pcd*.

### Characterization of Cell Death in *Su* versus *sh2* Kernels

Based on viability staining it is apparent that *Su* endosperm cells die in a progression starting in the central portion of the kernel between 16 and 20 dap, proceeding toward the cap by 24 dap and eventually toward the base of the kernel between 28 and 40 dap. The timing and progression of this process is similar to that of other processes, such as endoreduplication and starch deposition, that also occur during endosperm development (Shannon, 1974; Phillips et al., 1985; Kowles and Phillips, 1988; Doehler et al., 1994). In *sh2* endosperm cell death initiates earlier in the central endosperm and progresses outwardly more rapidly than in *Su* endosperm. Therefore, the timing of cell death in *sh2* endosperm occurs before the timing of reserve deposition in *Su* kernels and interferes with starch and storage protein synthesis in these cells.

The shrunken phenotype in *sh2* kernels results from the collapse of central endosperm cells and the subsequent formation of a large central cavity. During final maturation and desiccation, the outer starch-filled peripheral layers of the *sh2* endosperm collapse against the scutellum. These events are similar to those that occur during the development of *sh1* kernels, which, according to Chourey et al. (1991), also undergo premature cell degeneration in the central endosperm. These authors hypothesized that degeneration in *sh1* endosperm is due to either an osmotic imbalance as a result of the impaired Suc utilization or to deficient cellulose/hemicellulose content of cell walls as a result of reduced levels of UDP-Glc, the immediate reaction product of the Suc synthase 1 isozyme.

Alternatively, the premature cell degeneration in both of these starch-deficient mutants may result from the induction of cell wall-degrading enzymes in response to the elevated ethylene levels we found in *sh2* kernels. Ethylene is known to induce cell wall-hydrolyzing enzymes during a number of processes, including softening of climacteric fruits (Cass et al., 1990; Redgwell and Fry, 1993; MacLachlan and Brady, 1994), leaf and floral abscission (Jackson and Osborne, 1970), and formation of lysogenic aerenchyma in maize roots following exposure to hypoxic conditions (He et al., 1996; Saab and Sachs, 1996). This hypothesis could be tested by assaying the activity of cell wall-degrading enzymes during endosperm development in these and other starch-deficient endosperm mutants.

Internucleosomal DNA cleavage is one of several characteristic features of apoptosis (Wyllie et al., 1984; Wyllie, 1995) and has been demonstrated in both animals and plants during *pcd* (Mittler et al., 1995; Levine et al., 1996; Ryerson and Heath, 1996; Wang et al., 1996b). We demonstrated that internucleosomal DNA fragmentation occurs during endosperm development in both *Su* and *sh2* genotypes in two inbred backgrounds (II451b and Oh43). Furthermore, a greater extent of DNA fragmentation is associated with more rapid cell death and cellular degeneration and elevated ethylene production in *sh2* endosperm. Although *Su* endosperm cell death is evident by 16 dap, DNA ladders are not detected until approximately 12 d later. This discrepancy may be due in part to the low proportion of central cells undergoing DNA fragmentation at early developmental stages in the whole endosperms sampled. DNA fragmentation may indicate that cell death during maize endosperm development shares features commonly associated with apoptosis (Wyllie 1980; Earnshaw, 1995), although this is yet to be established.

Internucleosomal DNA cleavage has been shown to correlate with the activation of endogenous nuclear  $Ca^{2+}$ -dependent endonucleases well in advance of the loss in membrane integrity during apoptosis in animals (Wyllie, 1980; Arrends et al., 1990; Barry and Eastman, 1992; Collins et al., 1992). We have identified three nucleases, which we classify as nuclease I (EC 3.1.30.1) enzymes because they degrade both single-stranded DNA and RNA, are not active below pH 5.0, and are sensitive to EDTA. Nuclease activities are significantly higher in *sh2* endosperm between 20 and 36 dap compared with *Su* endosperm, possibly causing the more extensive DNA fragmentation. However, nuclease activity is also high in both the *Su* and *sh2* genotypes at early stages of development and declines to low levels by 24 dap. This early activity peak may represent *pcd* occurring in the nucellus, which is replaced by the rapidly growing endosperm by 12 dap (Kowles and Phillips, 1988), or it may be associated with the rapid cell division events occurring early in endosperm development.

A number of endosperm properties associated with starch-deficient mutants such as *sh2* and *su1se1* have been suggested to be important and interactive in contributing to poor germination. These include insufficient starch content and reduced endosperm to embryo ratios (Wann, 1980; Harris and DeMason, 1989; Azanza et al., 1996), reduced storage protein reserves (Tsai et al., 1978; Harris and DeMason, 1989), and limited starch hydrolysis due to reduced  $\alpha$ -amylase activity (Sanwo and DeMason, 1992, 1993; T.E. Young, J.A. Javik, and D.A. DeMason, unpublished data).

We found that the major developmental differences between *Su* and *sh2* kernels are in endosperm characteristics, which ultimately result in fewer reserve-filled cells. In addition, a number of embryo features have also been suggested to play minor roles in poor germination, especially in *sh2* genotypes. These include lower germination percentages and less vigorous growth under standard culture conditions (Styer and Cantliff, 1984; S.A. Novak and D.A. DeMason, unpublished data).

Parera et al. (1996) hypothesized that the poor growth of *sh2* embryos is due in part to defects in membrane integrity and membrane damage during imbibition, which results in higher electrolyte leakage. We found that small patches of scutellar cells die, accompanied by DNA fragmentation, during late *sh2* kernel development in one of the backgrounds (Il451b) and suggest that this abnormality could account for greater electrolyte leakage and reduced germination and growth rates of *sh2* embryos. The loss of membrane integrity and fragmentation of nDNA have also been shown to occur in rye seeds during prolonged storage and appear to be important factors contributing to delayed germination and loss of viability (Cheah and Osborne, 1978; Osborne, 1980). Scutellar cell death during *sh2* kernel development appears to be background specific, since it does not occur in Oh43.

### Role of Ethylene in Mediating Cell Death and DNA Fragmentation

ACC levels are highest in the high-sugar genotypes (*su1se1* and *sh2*) compared with the *Su* and *su1* genotypes in this set of isogenic lines. Moreover, there are two peaks in ACC content during kernel development, the first occurring 16 to 20 dap in all genotypes and the second 32 to 36 dap, which is predominant in the *sh2* genotype and less so in the *su1se1* genotype. The majority of ACC is found in the endosperm of both *Su* and *sh2* genotypes at early stages of development, whereas at later stages of development there are approximately equal amounts present in both the endosperm and embryo of the *sh2* genotype. The timing and extent of ethylene production closely parallel those of ACC content during kernel development, since two peaks occur at approximately the same time and elevated levels occur in the *su1se1* and *sh2* genotypes relative to *Su* and *su1* genotypes. These data correlate well with the more rapid and extensive cell death occurring in the *sh2* endosperm. To our knowledge, this is the first report implicating ethylene as a potential mediator of the pleiotropic effects associated with abnormal endosperm development of starch-deficient mutants of maize.

Despite the generally good correlation between ACC content and ethylene production, some discrepancies are evident. For example, *sh2* kernels of Il451b contain 20 times more ACC 36 dap than do *Su* kernels, whereas ethylene production is only 5 times as high in *sh2* kernels compared with *Su* kernels. Similarly, *su1* kernels possess ethylene production rates comparable to those of the *su1se1* genotype and yet contain very low ACC levels during late kernel development. The low ACC levels present during late endosperm development of *Su* and *su1* genotypes may reflect conversion to conjugated forms such as malonyl-ACC or glutamyl-ACC as a means of sequestering ACC either to prevent its conversion to ethylene or to control the rate of this process (Amrhein et al., 1981; Jiao et al., 1986; Hanley et al., 1989; Martin et al., 1995). We currently have no information concerning the amount of conjugated forms of ACC present during maize endosperm development.

When comparing ethylene production in *Su* and *sh2* kernels between two inbred backgrounds, we observed

that overall ethylene production rates were higher in the Oh43 background compared with Il451b, which may in part be due to the larger kernel size of Oh43 (approximately 33% greater). We also observed that relative differences between *Su* and *sh2* kernels of Oh43 were less than those in Il451b. These data suggest that elevated ethylene production in the *sh2* compared with wild-type kernels can be modified depending on the genetic background, and these relative differences may in part determine the severity of the pleiotropic effects ascribed to the mutation.

Exogenous ethylene application to developing *Su* and *sh2* kernels results in earlier and more extensive cell death in the endosperm and is accompanied by more extensive DNA fragmentation in all genotypes and inbred lines tested, thereby establishing a causal relationship between ethylene production and the abnormal *sh2* kernel development. Conversely, treatment with AVG reduces cell degeneration, cavity formation within the central endosperm, and DNA fragmentation during *sh2* kernel development. AVG treatments reduced ethylene production to levels normally found within *Su* kernels but was not sufficient to eliminate cell death or DNA fragmentation. Higher concentrations may be capable of delaying or reducing the progression of pcd. Collectively, these data suggest that ethylene is involved in the signal transduction pathway leading to pcd of starchy endosperm cells, and they support the hypothesis that ethylene is the signal responsible for the premature cell death and greater degree of DNA fragmentation observed in developing *sh2* kernels.

We note that the exogenous application of ethylene to developing maize kernels results in the death and collapse of endosperm cells in a progression from the outside toward the center (centripetally), which is the opposite of the normal centrifugal progression. We hypothesize that ethylene is normally synthesized first within the central endosperm and then proceeds outward as the endosperm develops, similar to the observed progression of pcd. Temporal and spatial patterns of ethylene production during maize endosperm development could be determined by localizing ACC synthase or ACC oxidase mRNA. Alternatively, it is possible that the progression of cell death in response to ethylene may be determined by the timing and location of ethylene receptor synthesis within these cells, as has been shown during fruit ripening, flower senescence, and abscission in tomato (Payton et al., 1996). Currently, no ethylene receptors have been characterized in developing maize endosperm. However, distinguishing between these two possibilities could potentially be an important step in further elucidating the regulation of ethylene-mediated pcd during maize kernel development.

Associated with the premature endosperm cell death of Il451b (*Su*) kernels following ethylene exposure is a significant reduction in mature kernel dry weight to approximately 75% of control kernels. Beltrano et al. (1994) also showed that the application of ethylene to wheat ears hastened the process of grain maturation and resulted in a concurrent reduction in dry weight by approximately 12% of the control, whereas treatment with inhibitors of ethylene biosynthesis had the opposite effect. Taken together, these observations suggest that ethylene may play a fun-

damental role not only in maize endosperm *pcd* but in cereal kernel development in general.

Cell death in the scutellum and DNA fragmentation in embryos also results from exogenous ethylene treatment of *Su* kernels. This is similar to what was observed in Il451b *sh2* kernels during normal development and supports the hypothesis that excessive ethylene production during kernel development is responsible for the abnormal scutellum phenotype observed in this background. Moreover, we observed a significant reduction in the percentage of germination of ethylene-treated kernels to approximately 5% of control kernels, although the cause of this reduced germination or the extent to which these effects are associated with either the endosperm or embryo are unknown.

### Basis of Ethylene Production during Kernel Development

Starch-deficient endosperm mutations of maize, such as *sh2*, result in elevated endosperm Suc content during kernel development (Creech, 1965; Boyer and Shannon, 1983). Elevated sugar content and/or reduced water potential may be the primary signal responsible for elevated ethylene production in these mutants. However, there is limited information about the possible mechanism by which this could occur. The presence of two ethylene peaks during kernel development is common to all of the lines tested. This biphasic pattern may be controlled in part by other developmentally and/or stress-induced hormones.

Auxins and cytokinins are capable of stimulating ethylene production in a wide variety of plant tissues (Morgan and Hall, 1962; Fuchs and Lieberman, 1968; Lau and Yang, 1973; Yeong-Biau and Yang, 1979). Furthermore, Philosoph-Hadas et al. (1984) reported that treatment of tobacco leaf discs with Suc, Gal, or Glc could stimulate both ACC and ethylene production and acted in synergism with IAA. Auxin has also been implicated in directing the process of cereal grain development and occurs as two peaks, the first between 9 and 11 dap and the second 20 dap (Rademacher and Graebe, 1984; Mengel et al., 1985; Lee et al., 1989; Lur and Setter, 1993). Methyl jasmonate has been shown to be effective in stimulating ethylene biosynthesis during tomato fruit ripening and in detached rice leaves (Saniewski et al., 1987a, 1987b; Chou and Kao, 1992). Furthermore, Lehmann et al. (1995) showed that treatment of barley leaf segments with sorbitol, Glc, or other sugars could significantly increase the production of jasmonic acid and methyl jasmonate. Moreover, the levels of ethylene and jasmonic acid influence each other during the wound response in tomato plants (O'Donnell et al., 1996). Although jasmonic acid and methyl jasmonate are widely occurring plant growth substances (Meyer et al., 1984), further work is needed to determine the extent to which auxin or methyl jasmonate might induce ethylene production in developing maize endosperm.

In our characterization of maize endosperm development in *Su* and *sh2* kernels, we implicate ethylene in the *pcd* signal transduction pathway. Moreover, we identify ethylene as the signal involved in mediating the pleiotropic effects on endosperm development in starch-deficient endosperm mutants of maize. In light of these results, we

propose that modifying ethylene biosynthesis may provide a potential means for improving the development and possibly the germination of *sh2* and *su1se1* genotypes. By understanding more fully the impact of ethylene on maize endosperm development and the potential interactions with other hormones, it may be possible to modify endosperm dry matter accumulation or quality in maize and other cereals.

### ACKNOWLEDGMENTS

The authors would like to thank Drs. Julia Bailey-Serres and Timothy Close for critical review of this manuscript. We would also like to thank Janet Giles for technical assistance with light microscopy of maize kernels and Dr. Ursula Schuch and Darren Haver for assistance with ethylene determination.

Received April 14, 1997; accepted June 26, 1997.

Copyright Clearance Center: 0032-0889/97/115/0737/15.

### LITERATURE CITED

- Abeles FB, Morgan PW, Saltveit ME Jr (1992) Ethylene in Plant Biology. Academic Press, San Diego, CA
- Amrhein N, Schneebeck D, Skoripka H, Tophof S, Stockigt J (1981) Identification of a major metabolite of the ethylene precursor 1-aminocyclopropane-1-carboxylic acid in higher plants. *Naturwissenschaften* 68: 619-620
- Apte SS, Mattei M-G, Seldin MF, Olsen BR (1995) The highly conserved defender against the death 1 (DAD1) gene maps to human chromosome 14q11-q12 and mouse chromosome 14 and has plant and nematode homologs. *FEBS Lett* 363: 304-306
- Arrends MJ, Morris RG, Wyllie AH (1990) Apoptosis—the role of the endonuclease. *Am J Pathol* 136: 593-608
- Azanza F, Bar-Zur A, Juvik JA (1996) Variation in sweet corn kernel characteristics associated with stand establishment and eating quality. *Euphytica* 87: 7-18
- Bachmair A, Becker F, Masterson RV, Schell J (1990) Perturbation of the ubiquitin system causes leaf curling, vascular tissue alterations and necrotic lesions in a higher plant. *EMBO J* 9: 4543-4549
- Barry MA, Eastman A (1992) Endonuclease activation during apoptosis: the role of cytosolic  $Ca^{2+}$  and pH. *Biochem Biophys Res Commun* 186: 782-789
- Beltrano J, Carbone A, Montaldi ER, Guamet JJ (1994) Ethylene as promoter of wheat grain maturation and ear senescence. *Plant Growth Regul* 15: 107-112
- Bhave MR, Lawrence S, Barton C, Hannah LC (1990) Identification and molecular characterization of *shrunk2-2* cDNA clones of maize. *Plant Cell* 2: 581-588
- Boyer CD, Shannon JC (1983) The use of endosperm genes for sweet corn quality improvement. *Plant Breed Rev* 1: 139-161
- Bradford MM (1976) A rapid and sensitive method for the quantitation of microgram quantities of protein utilizing the principle of protein-dye binding. *Anal Biochem* 72: 248-254
- Campbell R, Drew MC (1983) Electron microscopy of gas space (aerenchyma) formation in adventitious roots of *Zea mays* L. subjected to oxygen shortage. *Planta* 157: 350-357
- Cass LG, Kirven KA, Christoffersen RE (1990) Isolation and characterization of a cellulase gene family member expressed during avocado fruit ripening. *Mol Gen Genet* 223: 76-86
- Chasan R (1994) Tracing tracheary element development. *Plant Cell* 6: 917-919
- Cheah KSE, Osborne DJ (1978) DNA lesions occur with loss of viability in embryos of aging rye seed. *Nature* 272: 593-599
- Chen Y-G, Chourey PS (1989) Spatial and temporal expression of the two sucrose synthase genes in maize: immunohistological evidence. *Theor Appl Genet* 78: 553-559



- Chou CM, Kao CH** (1992) Stimulation of 1-aminocyclopropane-1-carboxylic acid-dependent ethylene production in detached rice leaves by methyl jasmonate. *Plant Sci* **83**: 137-141
- Chourey PS, Chen Y-C, Miller ME** (1991) Early cell degeneration in developing endosperm is unique to the *shrunken* mutation in maize. *Maydica* **36**: 141-146
- Collins RJ, Harmon BV, Gobe GC, Kerr JFR** (1992) Internucleosomal DNA cleavage should not be the sole criterion for identifying apoptosis. *Int J Radiat Biol* **61**: 451-453
- Concepcion M, Lizada C, Yang SF** (1979) A simple and sensitive assay for 1-aminocyclopropane-1-carboxylic acid. *Anal Biochem* **100**: 140-145
- Creech RG** (1965) Genetic control of carbohydrate synthesis in maize endosperm. *Genetics* **52**: 1175-1186
- DeMason DA** (1994) Controls of germination in noncereal monocotyledons. *Adv Struct Bio* **3**: 285-310
- Dietrich RA, Delaney TP, Uknes SJ, Ward ER, Ryals JA, Dangel JL** (1994) *Arabidopsis* mutants simulating disease resistance response. *Cell* **77**: 565-577
- Doehler DC, Smith LJ, Duke ER** (1994) Gene expression during maize kernel development. *Seed Sci Res* **4**: 299-305
- Douglass SK, Juvik JA, Splittstoesser WE** (1993) Sweet corn seedling emergence and variation in kernel carbohydrate reserves. *Seed Sci Technol* **21**: 433-445
- Drew MC, Jackson MB, Giffard S** (1979) Ethylene-promoted adventitious rooting and development of cortical air spaces (aerenchyma) in roots may be adaptive response to flooding in *Zea mays* L. *Planta* **147**: 83-88
- Earnshaw WC** (1995) Apoptosis: lessons from in vitro systems. *Trends Cell Biol* **5**: 217-220
- Esau K** (1977) *Seed Plant Anatomy*, Ed 2. Academic Press, NY
- Ferguson JE, Dickinson DB, Rhodes AM** (1979) Analysis of endosperm sugars in a sweet corn inbred (Illinois 677a) which contains the *sugary enhancer1 (sulsel1)* gene and comparison of *sulsel1* with other corn genotypes. *J Plant Physiol* **63**: 416-420
- Fisher DB** (1968) Protein staining of ribboned Epon sections for light microscopy. *Histochemistry* **16**: 92-96
- Fluhr R, Mattoo AK** (1996) Ethylene-biosynthesis and perception. *Crit Rev Plant Sci* **15**: 479-523
- Fuchs Y, Lieberman M** (1968) Effects of kinetin, IAA, and gibberellin on ethylene production, and their interactions in growth of seedlings. *Plant Physiol* **43**: 2029-2036
- Gaff DF, Okong 'O-Ogola O** (1971) The use of non-permeating pigments for testing the survival of cells. *J Exp Bot* **22**: 756-758
- Gerschenson LE, Totello RJ** (1992) Apoptosis: a different type of cell death. *FASEB J* **6**: 2450-2455
- Gonzales JW, Rhodes AM, Dickinson DB** (1976) Carbohydrate and enzymatic characterization of a high sucrose inbred line of sweet corn. *J Plant Physiol* **58**: 28-32
- Greenberg JT** (1996) Programmed cell death: a way of life for plants. *Proc Natl Acad Sci USA* **93**: 12094-12097
- Greenberg JT, Ausubel FM** (1993) *Arabidopsis* mutants compromised for the control of cellular damage during pathogenesis and aging. *Plant J* **4**: 327-341
- Greenberg JT, Guo A, Klessig DF, Ausubel FM** (1994) Programmed cell death in plants: a pathogen-triggered response activated coordinately with multiple defense functions. *Cell* **77**: 551-563
- Hanley KM, Meir S, Bramlage WJ** (1989) Activity of aging carnation flower parts and the effects of 1-(malonylamino)cyclopropane-1-carboxylic acid-induced ethylene. *Plant Physiol* **91**: 1126-1130
- Hannah LC, Nelson OE Jr** (1976) Characterization of ADP-glucose pyrophosphorylase from *shrunken-2* and *brittle-2* mutants of maize. *Biochem Genet* **14**: 547-560
- Harris MJ, DeMason DA** (1989) Comparative kernel structure of three endosperm mutants of *Zea mays* L. relating to seed viability and seedling vigor. *Bot Gaz* **150**: 50-62
- He C-J, Morgan PW, Drew MC** (1996) Transduction of an ethylene signal is required for cell death and lysis in the root cortex of maize during aerenchyma formation induced by hypoxia. *Plant Physiol* **112**: 463-472
- Hengartner MO, Horvitz HR** (1994) The ins and outs of programmed cell death during *C. elegans* development. *Philos Trans R Soc Lond-Biol Sci* **345**: 243-246
- Jackson MB, Osborne DJ** (1970) Ethylene, the natural regulator of leaf abscission. *Nature* **225**: 1019-1022
- James MG, Robertson DS, Meyers AM** (1995) Characterization of the maize gene *sugary1*, a determinant of starch composition in kernels. *Plant Cell* **7**: 417-429
- Jiao X-Z, Philosoph-Hadas S, Su L-Y, Yang SF** (1986) The conversion of 1-(malonylamino)cyclopropane-1-carboxylic acid to 1-aminocyclopropane-1-carboxylic acid in plant tissues. *Plant Physiol* **81**: 637-671
- Kerr JFR, Gobe GC, Winterford CM, Harmon BV** (1995) Anatomical methods in cell death. *Methods Cell Biol* **46**: 1-27
- Kowles RV, Phillips RL** (1988) Endosperm development in maize. *Int Rev Cytol* **112**: 97-136
- Kyle DJ, Styles ED** (1977) Development of aleurone and sub-aleurone layers in maize. *Planta* **137**: 185-193
- Lamb CJ** (1994) Plant disease resistance genes in signal perception and transduction. *Cell* **76**: 419-422
- Lau OL, Yang SF** (1973) Mechanism of a synergistic effect of kinetin on auxin-induced ethylene production: suppression of auxin conjugation. *Plant Physiol* **51**: 1011-1014
- Lee B, Martin P, Bangerth F** (1989) The effect of sucrose on the levels of abscisic acid, indoleacetic acid and zeatin/zeatinriboside in wheat ears growing in liquid culture. *Physiol Plant* **77**: 73-80
- Lehmann J, Atzorn R, Bruchner C, Reinbothe S, Leopold J, Wasternack C, Parthier B** (1995) Accumulation of jasmonate, abscisic acid, specific transcripts and proteins in osmotically stressed barley leaf segments. *Planta* **197**: 156-162
- Levine A, Pennell RI, Alvarez ME, Palmer R, Lamb C** (1996) Calcium-mediated apoptosis in a plant hypersensitive disease resistance response. *Curr Biol* **6**: 427-437
- Lopes MA, Larkins BA** (1993) Endosperm origin, development, and function. *Plant Cell* **5**: 1383-1399
- Lur H-S, Setter TL** (1993) Role of auxin in maize endosperm development. *Plant Physiol* **103**: 273-280
- Maclachlan G, Brady C** (1994) Endo-1,4- $\beta$  glucanase, xyloglucanase, and xyloglucan endo-transglycosylase activities versus potential substrates in ripening tomatoes. *Plant Physiol* **105**: 965-974
- Martin MN, Cohen JD, Saftner RA** (1995) A new 1-aminocyclopropane carboxylic acid-conjugating activity in tomato fruit. *Plant Physiol* **109**: 917-926
- Mattoo AK, Suttle CS** (1991) *The Plant Hormone Ethylene*. CRC Press, Boca Raton, FL
- Mengel K, Friedrich B, Judel GK** (1985) Effect of light intensity on the concentrations of phytohormones in developing wheat grains. *J Plant Physiol* **120**: 255-266
- Meyer A, Miersch O, Buttner C, Sembdner G, Schreiber K** (1984) Occurrence of the plant growth regulator jasmonic acid in plants. *J Plant Growth Regul* **3**: 1-8
- Mittler R, Shulaev V, Lam E** (1995) Coordinate activation of programmed cell death and defense mechanisms in transgenic tobacco plants expressing a bacterial proton pump. *Plant Cell* **7**: 29-42
- Morgan PW, Hall WC** (1962) Effect of 2,4-dichlorophenoxyacetic acid on the production of ethylene by cotton and grain sorghum. *Plant Physiol* **15**: 420-427
- O'Brien TP, McCully ME** (1981) *The Study of Plant Structure: Principals and Selected Methods*. Termarcarphi Pty., Melbourne, Australia
- O'Donnell PJ, Calvert C, Atzorn R, Wasternack C, Leyser HMO, Bowles DJ** (1996) Ethylene as a signal mediating the wound response of tomato plants. *Science* **274**: 1914-1917
- Osborne DJ** (1980) Senescence in seeds. In KV Thinmann, ed, *Senescence in Plants*. CRC Press, Boca Raton, FL, pp 13-37
- Pan D, Nelson OE** (1984) A debranching enzyme deficiency in endosperms of the *sugary-1* mutants of maize. *Plant Physiol* **74**: 324-328

- Parera CA, Cantliff DJ, McCarty DR, Hannah LC** (1996) Improving vigor in shrunken2 corn seedlings. *J Am Soc Hortic Sci* **121**: 1069–1075
- Payton S, Fray RG, Brown S, Grierson D** (1996) Ethylene receptor expression is regulated during fruit ripening, flower senescence and abscission. *Plant Mol Biol* **31**: 1227–1231
- Phillips RL, Kowles RV, McMullen M, Enomoto S, Rubenstein I** (1985) Developmentally timed changes in maize endosperm DNA. In M Freeling, ed, *Plant Genetics*. Alan R. Liss, New York, pp 739–754
- Philosoph-Hadas S, Meir S, Aharoni N** (1984) Characterization of the carbohydrate-stimulated ethylene production in tobacco leaf discs. In Y Fuchs, E Chalutz, eds, *Ethylene: Biochemical, Physiological and Applied Aspects*. Martinus Nijhoff/Dr W Junk Publishers, The Hague, pp 95–96
- Rademacher W, Graebe JE** (1984) Hormonal changes in developing kernels of two spring wheat varieties differing in storage capacity. *Ber Dtsch Bot Ges* **97**: 167–181
- Redgwell RJ, Fry SC** (1993) Xyloglucan endotransglycosylase activity increases during kiwifruit (*Actinidia deliciosa*) ripening. *Plant Physiol* **103**: 1399–1406
- Ryerson DE, Heath MC** (1996) Cleavage of nuclear DNA into oligonucleosomal fragments during cell death induced by fungal infection or by abiotic treatments. *Plant Cell* **8**: 393–402
- Saab IN, Sachs MM** (1996) A flooding-induced xyloglucan endotransglycosylase homologue in maize is responsive to ethylene and associated with aerenchyma. *Plant Physiol* **112**: 385–391
- Saniewski M, Nowacki J, Czapski J** (1987a) The effect of methyl jasmonate on ethylene production and ethylene-forming enzyme activity in tomatoes. *J Plant Physiol* **129**: 175–180
- Saniewski M, Urbanek H, Czapski J** (1987b) Effect of methyl jasmonate on ethylene production, chlorophyll degradation, and polygalacturonase activity in tomatoes. *J Plant Physiol* **127**: 177–181
- Sanwo MM, DeMason DA** (1992) Characteristics of  $\alpha$ -amylase during germination of two high-sugar sweet corn cultivars of *Zea mays* L. *Plant Physiol* **99**: 1184–1192
- Sanwo MM, DeMason DA** (1993) A comparison of  $\alpha$ -amylase isozyme profiles in selected *Su* and high-sugar sweet corn (*sh2*, *su1*, *su1se1*) lines (*Zea mays* L.). *Int J Plant Sci* **154**: 395–405
- Shannon JC** (1974) *In vivo* incorporation of carbon-14 into *Zea mays* L. starch granules. *Cereal Chem* **51**: 798–809
- Styer RC, Cantliff DJ** (1983) Changes in seed structure and composition during development and their effects on leakage in two endosperm mutants of sweet corn. *J Am Soc Hortic Sci* **108**: 717–720
- Styer RC, Cantliff DJ** (1984) Dependence of seed vigor during germination on carbohydrate source in endosperm mutants of maize. *Plant Physiol* **76**: 196–200
- Sugimoto A, Hozak RR, Nakashima T, Nishimoto T, Rothman J** (1995) *dad-1*, an endogenous programmed cell death suppressor in *Caenorhabditis elegans* and vertebrates. *EMBO J* **14**: 4434–4441
- Thelen MP, Northcote DH** (1989) Identification and purification of a nuclease from *Zinnia elegans* L.: a potential marker for xylogenesis. *Planta* **179**: 181–195.
- Tomei LD, Cope FO (eds)** (1991) *Apoptosis: The Molecular Basis of Cell Death*. Cold Spring Harbor Laboratory Press, Cold Spring Harbor, NY
- Tomei LD, Cope FO (eds)** (1994) *Apoptosis II: The Molecular Basis of Apoptosis in Disease*, Current Communications in Cell and Molecular Biology. Cold Spring Harbor Laboratory Press, Cold Spring Harbor, NY
- Tsai CY, Larkins BA, Glover DV** (1978) Interaction of the *opaque2* gene with starch-forming mutant genes of the synthesis of zein in maize endosperm. *Biochem Genet* **16**: 883–896
- Wang H, Bostock RM, Gilchrist DG** (1996a) Apoptosis: a functional paradigm for programmed cell death induced by a host-selective phytotoxin and invoked during development. *Plant Cell* **8**: 375–391
- Wang M, Oppedijk BJ, Lu X, Van Duijn B, Schilperoort RA** (1996b) Apoptosis in barley aleurone during germination and its inhibition by abscisic acid. *Plant Mol Biol* **32**: 1125–1134
- Wann E** (1980) Seed vigor and respiration of maize kernels with different endosperm genotypes. *J Am Soc Hortic Sci* **105**: 31–34
- Ward ER, Uknes SJ, Williams SC, Dincher SS, Wiederhold DL, Alexander DC, Ahl-Goy P, Metraux JP, Ryals JA** (1991) Coordinate gene activity in response to agents that induce systemic acquired resistance. *Plant Cell* **3**: 1085–1094
- Wyllie AH** (1980) Cell death: the significance of apoptosis. *Int Rev Cytol* **68**: 251–306
- Wyllie AH** (1995) The genetic regulation of apoptosis. *Curr Opin Genet Dev* **5**: 97–104
- Wyllie AH, Morris RG, Smith AL, Dunlop D** (1984) Chromatin cleavage in apoptosis: association with condensed chromatin morphology and dependence on macromolecular synthesis. *J Pathol* **142**: 67–77
- Yeong-Biau Y, Yang SF** (1979) Auxin-induced ethylene production and its inhibition by aminoethoxyvinylglycine and cobalt ion. *Plant Physiol* **64**: 1074–1077